Command to Line-of-Sight Guidance: A Stochastic Optimal Control Problem

J.E. Kain*
The Analytical Sciences Corporation, Reading, Mass.
and
D.J. Yost†
Johns Hopkins University, Laurel, Md.

A command to line-of-sight (CLOS) guidance design approach using modern stochastic optimal control theory is discussed. CLOS guidance requires a wide guidance bandwidth in order to follow a threat maneuver. Yet the LOS noise (beam jitter) inherent in any LOS tracking scheme must be attenuated in order to prevent excessive control surface saturation. The stochastic describing function (CADET) is used to model the aerodynamic control surface saturation nonlinearity allowing the "linear" stochastic optimal control theory to be applied. Results from a sample airframe indicate near-optimal performance using a realizable nonlinear guidance compensation against a randomly maneuvering threat.

Introduction

A NAVAL point defense intercept scenario is depicted in Fig. 1. An incoming maneuvering missile threat is to be intercepted. The threat likely will be maneuvering in a stationary fashion about some line-of-sight trajectory to the impact point in the airspace near the ship. This type of maneuver will maximize threat maneuver effectiveness against the shipboard point defense weapons.

The control problem to be addressed here is one of guiding the defensive missile so as to intercept the attacking threat using only line-of-sight measurements from the interceptor launch point. Command to line-of-sight guidance, because of the simplicity of implementation, was one of the earliest forms of intercept guidance policies. Proportional navigation, which attempts to null the interceptor/threat line-of-sight rate, is known to provide better performance with less control effort in constant-velocity intercepts and is widely accepted as the preferred method of guidance. Nevertheless, a renewed emphasis on simplicity, reliability, low cost, and countermeasure invulnerability, along with advances in beam-pointing technology, has lead to renewed interest in this guidance method.

An additional argument in favor of the ship/threat line-of-sight measurement over the interceptor/threat line-of-sight measurement can be made based on the nature of the point defense threat. A proportional navigation guidance policy is well suited to intercept scenarios, where the threat heading is unknown but likely to be constant during homing. In this case, a lead angle can be computed based on instantaneous interceptor/threat line-of-sight rate so that intercept can occur with minimal interceptor acceleration. The point defense threat is unique in that the threat destination is assumed to be near the interceptor launch point. Thus we can predict with considerable certainty that the threat heading always will return to lie along the ship/threat line-of-sight. We can make use of this information by forcing the interceptor to fly "near" the ship-to-threat line-of-sight. In fact, a point defense interceptor using proportional navigation may tend to overreact to threat feinting maneuvers. A comparison of proportional navigation performance with the optimal CLOS guidance is given later.

A variety of "optimal" intercept guidance policies have been proposed in recent years as a result of the increasing acceptance of modern control theory. Because of the noise associated with line-of-sight measurements and the randomness of the likely threat maneuvers, the intercept problem

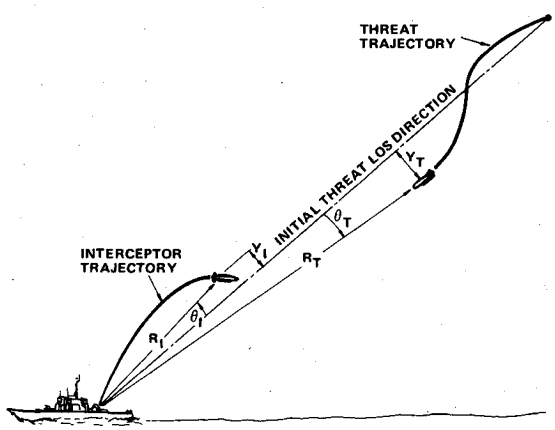

Fig. 1 Point defense intercept scenario.

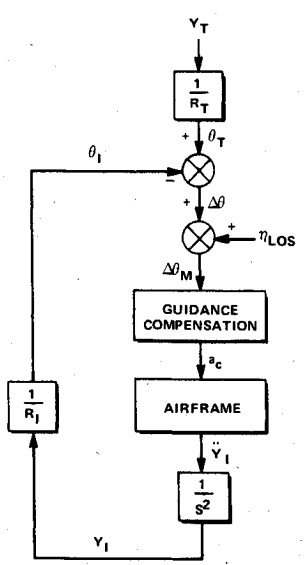

Fig. 2 Command to line-of-sight guidance loop.

Presented as Paper 76-1956 at the AIAA Guidance and Control Conference, San Diego, Calif., Aug. 16-18, 1976 (in bound volume of Conference papers); submitted Sept. 9, 1976; revision received Jan. 31, 1977.

Index categories: LV/M Dynamics and Control; LV/M Guidance; Missile Systems.

*Member of the Technical Staff. Member AIAA.
†Applied Physics Laboratory, Senior Staff. Member AIAA.

seems an excellent candidate for the stochastic optimal control methods. References 1 and 2 give a comparison of several such intercept policies for missiles with line-of-sight rate measurements.

Two major drawbacks to the practical application of such guidance policies to future missiles have been observed. First, these optimal strategies may be highly "tuned" to the system parameters assumed in the optimal control design. Sensitivity to off-nominal parameter variations and modeling errors may be unacceptable. Secondly, optimal intercept strategies usually require knowledge of time-to-go. Time-to-go implies knowledge of range-to-go, which in most cases implies radar ranging. An effective "passive" guidance policy that does not require threat range is more desirable.

Because of the nature of the ship/threat line-of-sight measurement, the command to line-of-sight (CLOS) guidance problem can be formulated as an optimal stochastic regulator problem. This allows the determination of control gains based only on time-into-flight. In addition, the known well-behaved closed-loop response of the optimal regulator insures a degree of parameter insensitivity.

An aerodynamic control surface limit or acceleration command limit must be included in the model for any highly maneuverable interceptor. Knowledge that a well-designed guidance policy likely will accelerate "to the limit" to reduce miss distance makes the application of the linear stochastic optimization theory questionable. Reference 2 derives the nonlinear optimal control law for the case where the control is restricted only in its upper bound for the sample data-control problem. The control law for this case can be summarized as follows. First solve for the constant control level required over the next sample period to null the predicted miss at the known final time. Prediction is accomplished via the Kalman filter and predictor. Clip this computed acceleration level at the limit value.

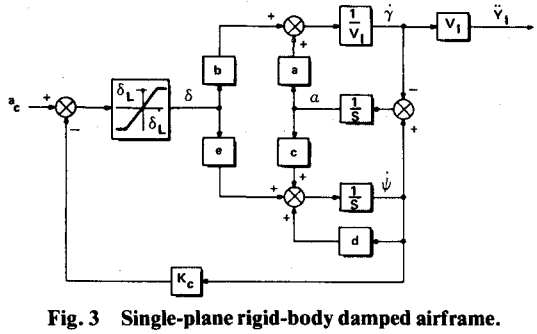

Fig. 3 Single-plane rigid-body damped airframe.

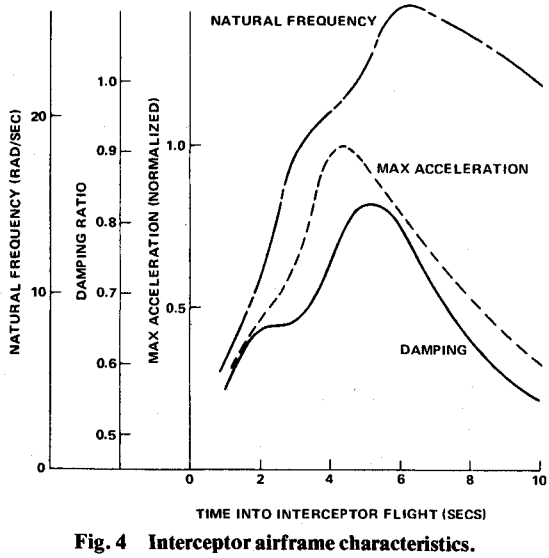

Fig. 4 Interceptor airframe characteristics.

Such a control policy produces considerable control fluctuation when compared with more traditional guidance laws and high control gains through-out the intercept. As indicated in Ref. 1, considerable parameter sensitivity results. Nevertheless, this approach may be useful for comparative purposes.

The approach for dealing with the nonlinearity presented herein allows the application of both the hard limit and the soft limit imposed by including a weighted integral of the control within the cost function. This method can be used to penalize the control "chattering," which can result when no integral control penalty is imposed.

The covariance analysis describing fuction technique (CADET) described in Refs. 3 and 4 is used to "linearize" the saturation nonlinearity statistically so that the linear optimal control theory can be applied.

The purpose of this paper is twofold. First we wish to present an efficient design tool for a realistic missile-guidance problem. Second, we wish to demonstrate how optimal stochastic control theory in conjunction with the stochastic describing function can be used to generate a nonlinear feedback control law.

Modeling the Intercept Problem

The command-to-LOS guidance loop can be approximated as shown in Fig. 2 using nomenclature defined in Fig. 1. The threat and interceptor displacements off the line-of-sight Y_T and Y_I are divided by the threat and interceptor ranges (R_T and R_I), respectively, to obtain the inertial LOS angles θ_T and θ_I. The measured pointing error $\Delta\theta_m$ is the input to the guidance compensator from which interceptor commands a_c are generated. The measured pointing error is corrupted by noise η_{LOS}, which for this study will be assumed wide in bandwidth with respect to the system characteristic frequencies.

Two types of measurement schemes for generating $\Delta\theta_m$ are used. For the "beamrider" guidance version, the threat is designated with a beam that is followed by the interceptor. The beam must be coded so as to provide the interceptor with off-LOS errors in two planes. In this case, the guidance compensator would be onboard the interceptor. Only a single tracker is required in this case, although the beam coding may be quite sophisticated. The second method tracks both the interceptor and threat and uplinks the appropriate guidance commands to the interceptor. The actual tracking in either case may be with infrared, rf, video, laser, etc., or various combinations. Both types of guidance schemes can be represented by Fig. 2. The noise magnitude will reflect the pointing accuracy for the particular system in use. A noise level of 0.0001 rad (0.1 mrad) will be assumed throughout this study.

An additional guidance input available in some systems is the threat range. Typically, range is measured by interpreting signals reflected from the threat. Interference signals can be generated by the threat and directed to the ship, making range measurements relatively vulnerable to electronic countermeasures. Note that threat directionality is more difficult to disguise. It will be assumed in the following discussion that threat range is unavailable for interceptor guidance purposes.

The single-plane, rigid-body interceptor airframe for this discussion will be modeled as in Fig. 3. The coefficients *a, b, c, d,* and *e* are the aerodynamic stability derivatives, V_I is the interceptor velocity, and K_c is the pitch-rate feedback gain. The aerodynamic control surface deflection δ must be limited to prevent control surface stall. The short-range point defense interceptor studied here attains maximum velocity and lateral acceleration capability about 5 sec after lauch at booster burnout. Lateral acceleration capability is reduced to about one-third of maximum at about 10 sec. Considerable airframe coefficient variation occurs during this time. The normalized characteristics of this airframe with K_c fixed are shown on

Fig. 4. These characteristics include the natural frequency ω_N, damping ζ, and maximum steady-state acceleration a_{max}.

The threat will be assumed to maneuver about the line-of-sight in a random fashion defined by the rms threat acceleration and the threat maneuver bandwidth. A stochastic representation of this threat will be generated by passing a white noise (η_T) through a third-order Butterworth filter (Fig. 5).

The threat displacement off the line-of-sight (Y_T) from this model is a stationary process, as is the threat acceleration ($\ddot{Y}_T$). The rms threat acceleration level can be used to specify the strength (spectral density) of the white noise input. The rms threat acceleration will be fixed at one-third the peak interceptor acceleration, whereas the threat maneuver bandwidth will be fixed at 1 rad/sec. A typical threat off-LOS trajectory generated by this process is shown on Fig. 6.

Guidance Compensation Design

The line-of-sight guidance loop of Fig. 2 typically is compensated using classical control theory. A multiplication by interceptor range (R_I) is assumed within the compensator (cancelling the $1/R_I$ in the feedback), the LOS noise is neglected, and a representative flight condition is selected. Also, the effects of control surface deflection limiting are not considered. The guidance loop becomes a linear time-invariant system and can be designed with the classical methods such as Bode analysis and root locus. A wide guidance loop bandwidth with acceptable phase and gain margin is the design objective.

In many cases, the LOS noise or beam jitter will dominate the interceptor performance. In addition to contributing directly to miss distance, noise (coupled with a wide guidance loop bandwidth) can cause performance deterioration because of saturation of the control surfaces. When control saturation is encountered, the closed-loop stability characteristics of the system will change from the linear theory predictions.

A guidance loop design procedure that directly addresses the problems of beam jitter and control surface limiting is required. Modern stochastic optimal control theory allows noise to be included in the design procedure, whereas the stochastic describing function (CADET) of Ref. 3 has been used successfully to model the saturation nonlinearity. By using the describing function with the linear optimal control theory, a useful design tool for the nonlinear command to line-of-sight guidance loop can be constructed.

Cost Function

A critical aspect of any optimal control problem is the cost function. For the intercept problem interceptor-threat range at some final time typically is minimized. In addition, the allowable control also must be penalized or limited to prevent unrealistic control motions. A cost function given by Eq. (1) frequently is used for intercept problems:

$$J_I = (Y_T - Y_I)^2 \Big|_{t_f} + u \int_0^{t_f} \delta^2 dt \qquad (1)$$

The miss distance is assumed to be the relative interceptor/threat separation off the line-of-sight ($Y_T - Y_I$) at the intercept time (t_f). The intercept time is assumed to be the time when interceptor and threat separation along the line-of-sight is zero, i.e., the time when $R_I = R_T$. The minimization of this cost function yields a tractable optimal control problem although the resulting gains will be a function not only of time into flight (t) but also time-to-go ($t_f - t$). Knowledge of time-to-go in this case implies knowledge of the threat range, which, as indicated earlier, is not a reliable measurement for guidance purposes.

We shall redefine the cost so as to obtain a "time-invariant" regulator solution based on a particular flight condition. The regulator solution will be obtained at successive discrete times along a nominal interceptor trajectory, yielding a smooth curve of optimal gains vs only time into flight. We shall proceed as in the classical analysis by assuming that the guidance compensator contains a multiplication by interceptor range. Thus the guidance loop of Fig. 2 can be redrawn as in Fig. 7.

Note in Fig. 7 that the interceptor off-beam displacement (Y_I) is controlled by the threat off-beam displacement (Y_T) only at intercept ($R_I = R_T$). Prior to the intercept time, the interceptor displacement is commanded proportionately less than the threat displacement. The stochastic optimal regulator will be designed based on the conditions at intercept. The guidance loop near intercept will be shown in Fig. 7, with $R_I = R_T$.

In effect, our guidance compensator gains always will be adjusted as though minimum distance off the LOS is desired at every point along the interceptor trajectory. Yet the input to the control loop will be attenuated by R_I/R_T, so that control effort is reduced when interceptor to threat range is large. This low level of control effort at large time-to-go is characteristic of the optimal control obtained by minimizing the cost of Eq. (1).

The stochastic regulator solution minimizes the cost function given by Eq. (2):

$$J = \lim_{t_f \to \infty} E\left[\int_0^{t_f} \{(Y_T - Y_I)^2 + \mu\delta^2\} d\tau\right] \qquad (2)$$

If the response time of the resulting guidance loop is "fast with respect to the variation of the airframe parameters, the resulting actual rms miss distance performance should be close to that predicted by the solution of the regulator problem. The selection of the control weighting μ requires some discussion. Through the use of this parameter, the optimization can be constrained in some manner. The weighting μ will, to some degree, control the bandwidth of the resulting guidance loop; i.e., a large μ will act to penalize control motions. If μ is set to zero, a bang-bang control will result (Ref. 5, p. 110) although the regulator solution becomes undefined and no convenient feedback control law can be computed. For the data presented here, a rather arbitary value of μ was selected which produced a reasonable amount of control limiting as predicted via CADET. This value was held constant for all regulator solutions discussed here. A more realistic approach is to select μ based on a specified amount of control limiting. It is likely that a sufficient degree of limiting will be encountered such that additional limiting produces negligible performance improvement.

Other constraints might be imposed by the appropriate selection of μ. For some interceptors, the net control energy available over the trajectory is limited because of battery lifetime, gas storage, etc. Rapid control surface motions

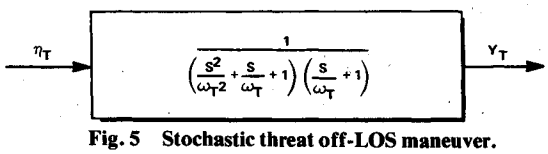

Fig. 5 Stochastic threat off-LOS maneuver.

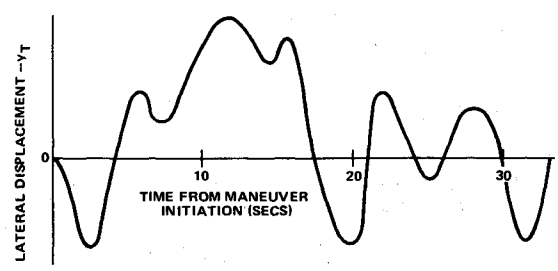

Fig. 6 Typical off-LOS displacement from the Butterworth threat model ($\omega_T = 1$ rad/sec).

between limits may be costly and can be controlled by μ. Another penalty paid by control motions is control-induced drag. The mean control-induced drag (D) can be approximated as $\bar{D}=aE(\alpha^2)$, where α is the angle of attack in radians, and a is normal force per angle of attack. This expression can be computed from the regulator solution and can be constrained using the weighting μ.

Optimal Stochastic Control Solution

Given the state description, measurement description, and cost function, the optimal control of a linear system is straightforward and well documented. The statistical linearization of a nonlinear system is derived in Ref. 6 and related to the describing function in Ref. 3, where it is called CADET. This statistical linearization allows the propagation of the system covariance matrix under the assumption that the joint state probability density remains gaussian. For a scalar input/scalar output nonlinearity imbedded in an otherwise linear system, CADET allows the replacement of the nonlinearity with a gain (describing function) computed from the mean and standard deviation of the nonlineariy input. Since the mean and covariance of the optimally controlled states are computed easily, the describing function linearization can be implemented within the stochasic optimal control solution. Further discussion of the statistical describing function use with the stochastic regulator can be found in Ref. 7.

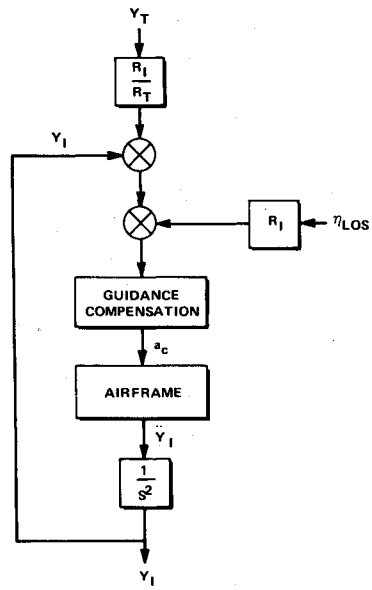

Fig. 7 CLOS guidance loop with range multiplication.

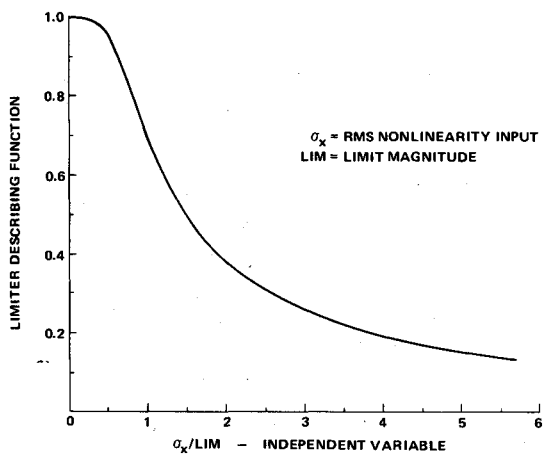

Fig. 8 Limiter-describing function for unbiased inputs.

Consider the following stochastic optimal control problem:

State Equation

$$\dot{x}=f(x,u)+\eta \tag{3}$$

Measurement Equation

$$y=Hx+\rho \tag{4}$$

Cost

$$J=E\left[\int_0^\infty (x^TAx+u^TBu)\,d\tau\right]$$

The spectral density of the process noise is given by the matrix Q, whereas the spectral density of the measurement noise is given as R. We shall assume that the resulting control and state will be zero mean. The following statistical linearization will be considered:[1,6]

$$\dot{x}=Fx+Gu+\eta \tag{6}$$

where

$$F=\frac{\partial}{\partial\bar{x}}E[f(x,u)] \tag{7}$$

$$G=\frac{\partial}{\partial\bar{u}}E[f(x,u)] \tag{8}$$

If x and u are assumed to be zero-mean, Gaussian random vectors, the expectations indicated in Eqs. (7) and (8) require only the covariance matrices of x and u.

The solutions of the stochastic regulator gains for the "linearized" problem defined by Eqs. (4-6) are given by the steady-state solution of the following Ricatti equations:

$$\dot{P}=FP+PF^T+Q-PHR^{-1}H^TP \tag{9}$$

$$\dot{S}=SF+F^TS+A-SGB^{-1}G^TS \tag{10}$$

$$K=PHR^{-1} \quad \text{(optimal estimator gains)} \tag{11}$$

$$C=B^{-1}GS \quad \text{(optimal control gains)} \tag{12}$$

The following equations will be used to approximate the optimal estimator-controller:

$$\dot{\hat{x}}=f(\hat{x},u)+K(y-H\hat{x}) \tag{13}$$

$$u=-C\hat{x} \tag{14}$$

This approach is somewhat different from that used in Ref. 7. Reference 7 suggests the use of the linearized state equation with the estimator, Eq. (13), rather than the nonlinear form. It is common practice to utilize the exact nonlinear dynamics to propagate the state estimate and yet design the estimator gains based on the linearized dynamics, as with the extended Kalman filter.

The following linear matrix equation is used frequently to compute the performance of the optimally controlled system[5]:

$$\dot{Z}=(F-GC)Z+Z(F-GC)^T+KRK^T \tag{15}$$

where

$$Z=E[\hat{x}\hat{x}^T] \tag{16}$$

$$P=E[(x-\hat{x})(x-\hat{x})^T] \tag{17}$$

$$Z+P=E[xx^T] \tag{18}$$

An apparent difficulty arises in the application of Eq. (15) to the evaluation of the optimal estimator-controller given by Eqs. (13) and (14). In the derivation of Eq. (13), the linearized matrix F associated with the actual system and the analogous

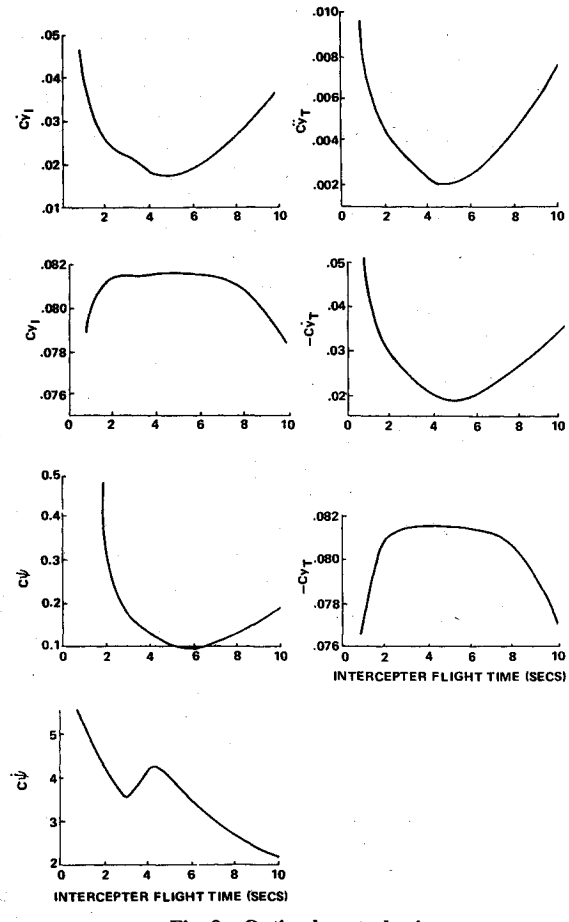

Fig. 9 Optimal control gains.

matrix associated with the estimator are assumed to be identical. Note that the statistical linearization of the optimal estimator is defined using the following gain matrices analogous to F and G:

$$F' = \frac{\partial}{\partial \hat{x}} E[f(\hat{x},u)] \tag{19}$$

$$G' = \frac{\partial}{\partial \bar{u}} E[f(\hat{x},u)] \tag{20}$$

The expectations indicated in Eqs. (19) and (20) are computed in terms of the covariance matrix of $\hat{x}$ rather than the covariance of x. For the problem considered here, the nonlinearity input is a combination of the control u and interceptor pitch rate state. The pitch rate estimate is not improved by the LOS measurement, and thus the variance of the pitch rate estimate is identical to the variance of the actual pitch rate. Therefore, the matrices F and G are identical to F' and G' for this problem. If this had not been the case, we would be required to utilize the Kalman filter sensitivity equations rather than Eq. (15), to evaluate the performance.

The steady-state solutions of Eqs. (9) and (10) were determined by simultaneously integrating Eqs. (9, 10, and 15) using Z and P to compute the matrices F and G. For the airframe dynamics depicted by Fig. 3, the describing function gain is used to replace the saturation nonlinearity in determing the linear system matrix F. The input to the limiter is the sum of the acceleration command (a_c) and the pitch rate feedback term. The acceleration command represents the control (u) in the preceding equations. When the rms limiter input is small with respect to the limit, the gain is near unity. The describing function gain vs rms input for the limiter is shown on Fig. 8 and derived in Ref. 8.

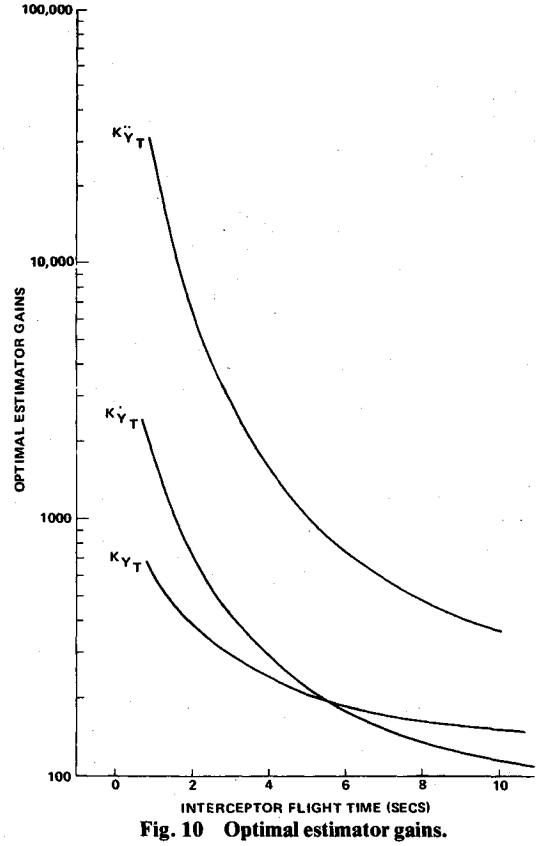

Fig. 10 Optimal estimator gains.

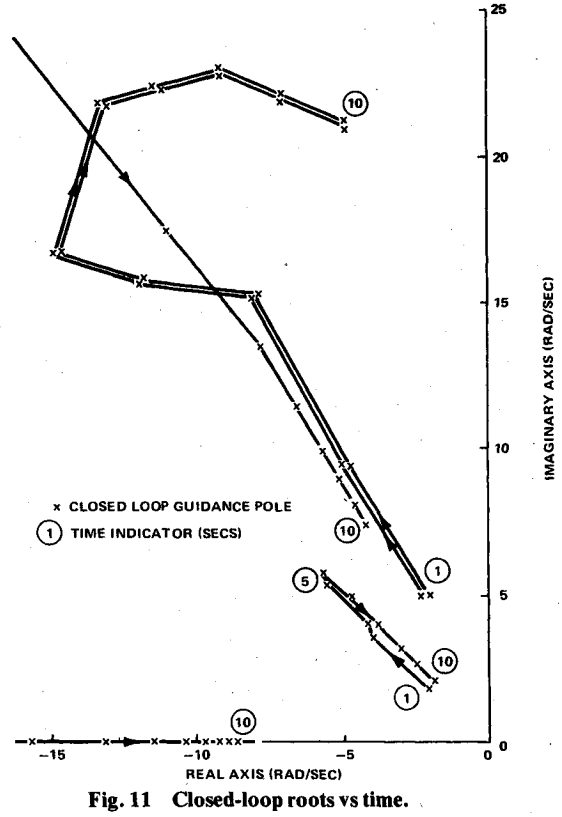

Fig. 11 Closed-loop roots vs time.

Guidance Compensator Solutions

The optimal stochastic regulator approximation just discussed was computed for the interceptor airframe and measurements discussed earlier. The state equations are

$$\ddot{Y}_T = -2\omega_T \ddot{Y}_T - 2\omega_T^2 \dot{Y}_T - \omega_T^3 Y_T + \eta_T \tag{21}$$

$$\ddot{Y}_I = a(\psi - \dot{Y}_I/V_I) + b \lim\{u + K_c\dot{\psi}\}. \tag{22}$$

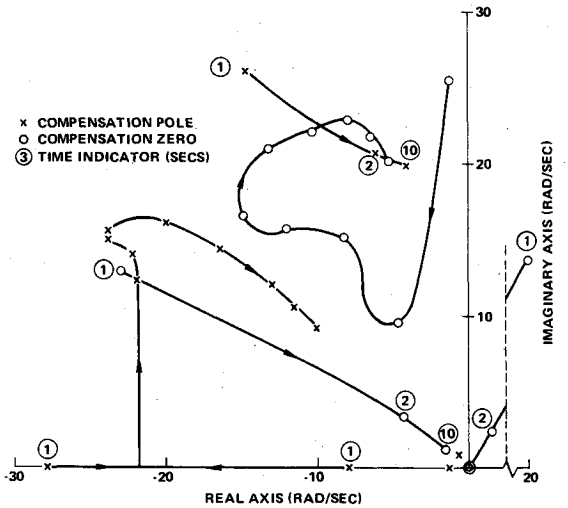

Fig. 12 Compensation pole-zero representation.

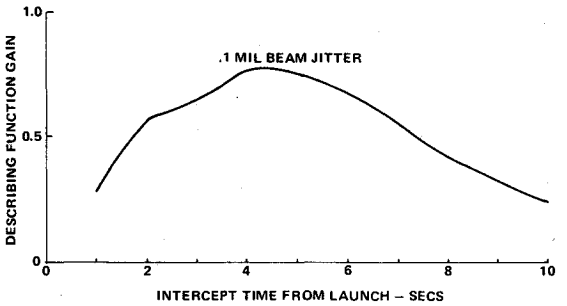

Fig. 13 Describing function gains from stochastic regulator solution.

$$\ddot{\psi} = c(\psi - \dot{Y}_I/V_I) + d\dot{\psi} + e \lim 8(u + K_c\dot{\psi}\} \qquad (23)$$

The measurement equation is

$$y = Y_T - Y_I + R_I(t)\eta_{\text{LOS}} \qquad (24)$$

and the cost is given by Eq. (2). These equations represent a seven-state, scalar control, scalar measurement nonlinear stochastic control problem.

The white measurement noise spectral density was selected to approximate a discrete uncorrelated process with sample time of 0.02 sec (Ref. 5, p. 342), i.e.,

$$Q = \sigma^2_{\text{LOS}} R_I^2(t)\, 0.02 \qquad (25)$$

The regulator problem was solved at 1-sec intervals along a nominal trajectory using a value of σ_{LOS} of 0.1 mrad. Gain histories from the regulator solutions are shown in Figs. 9 and 10. Figure 9 shows the seven optimal control gains, whereas Fig. 10 shows the estimator gains. All estimator gains are zero except those multiplying Y_T, $\dot{Y}_T$, $\ddot{Y}_T$. Recall that, for the optimal estimator solution, the control input is assumed effectively to be zero. Thus there are no stochastic inputs driving the interceptor states, resulting in zero steady-state gains for the interceptor state estimates. Solutions were obtained for a case where a correlated noise input was injected to the angle of attack (representative of a gust noise) although for realistic gust magnitudes the compensator and performance were unchanged.

If the nonlinearity is replaced by the describing function gain from the stochastic regulator design, a "linearized" system results, and concepts from linear system theory may be applied. Figure 11 shows the closed-loop system poles, whereas Fig. 12 shows the compensator poles. The pole travel is shown at 1-sec intervals into flight, beginning at 1 sec and ending at 10 sec. The resulting describing function gain history is shown on Fig. 13.

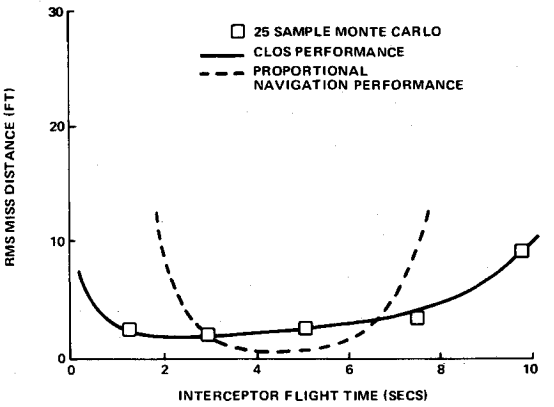

Fig. 14 Monte Carlo results.

For early flight times, the performance is dominated by the slow interceptor airframe response time, which results in a low guidance loop bandwidth. Late in flight, the system is dominated by the effects of LOS noise, and the resulting attenuation provided by the optimal system again produces a low guidance bandwidth. A peak bandwidth occurs at about 5 sec into flight and is about 8 rad/sec.

The guidance compensation indicated by Fig. 12 contains a double differentation, which cancels the double integration from the plant. The resulting system is thus "type 0" and has nonzero error to a bias input. A bias error on the LOS measurement easily could be included in the model and likely would lead to another compensation philosophy. In addition, a nonstationary target model (containing free integrators), which tends to turn from the LOS, would lead to a system with free integrations in the forward loop.

A considerable degree of control saturation is indicated by the describing function gains shown on Fig. 13. The value for the describing function gain gives an indication of the probability of the control surface *not* being limited for intercepts at the indicated time into flight.

Optimal System Performance

The previous section gave performance predictions based on two assumptions:

1) The airframe parameter time variations are slow with respect to the guidance loop bandwidth, allowing a "quasitime invariant" system design via the optimal regulator solution.

2) The describing function approximation is a valid characterization of the saturation nonlinearity.

Both assumptions are subject to question, since the airframe parameters vary rapidly, and a high degree of control limiting is predicted. The performance of the overall guidance system and the validity of the underlying assumptions were investigated using Monte Carlo methods. The airframe was simulated using a thorough aerodynamic description, and the saturation nonlinearity was modeled exactly in both the airframe and the guidance compensation. Twenty-five intercepts were flow against random threats generated from a digital representation of the Butterworth stochastic threat. Figure 14 shows the Monte Carlo results, together with the regulator solution rms miss distance prediction. All missile and target parameters are identical to those used in the guidance design procedure. The correlation between the Monte Carlo and the regulator prediction from Fig. 14 is excellent.

Also on Fig. 14 we show the performance of a proportional navigation guidance law using the previously discussed airframe. Time-varying gains were implemented to realize a navigation ratio of 3. A noiseless seeker was assumed although a 0.1-sec lag was inserted to represent guidance filtering and/or seeker lags. Figure 14 shows excellent per-

formance by the proportional navigation guidance when missile acceleration capability exceeds the rms threat acceleration by a factor of about 2, although performance degrades rapidly as the acceleration advantage is lost. Considerable performance improvement might be gained through the use of a more optimal law such as is presented in Ref. 2, although this would require gains programmed vs time-to-go. From Fig. 14, CLOS appears to offer considerable inner and outer boundary improvement over proportional navigation for the particular stationary threat considered here.

Conclusions

The CLOS guidance design procedure outlined here is a realistic alternative to the more classical approaches that ignore LOS noise characteristics and interceptor limiting. The design procedure is implemented easily and can be automated readily to allow rapid guidance redesign in response to propulsion modification, aerodynamic modifications, etc. The resulting guidance compensator structure is implemented easily either onboard the interceptor or within the shipboard fire control computer.

References

[1]Warren, R.S., Price, F.F., Gelb, A., and Vander Velde, W.E., "Direct Statistical Evaluation of Nonlinear Guidance Systems," AIAA Paper 73-836, Key Biscayne, Fla., Aug. 20-22, 1973.

[2]Deyst, J.J. and Price, C.F., "Optimal Stochastic Guidance Laws for Tactical Missiles," *Journal of Spacecraft and Rockets*, Vol. 10, May 1973, pp. 301-308.

[3]Gelb, A., and Warren, R.S., "Direct Statistical Analysis of Nonlinear Systems: CADET," *AIAA Journal*, Vol. 11, May 1973, pp. 689-694.

[4]Taylor, J.H., "Handbook for the Direct Statistical Analysis of Missile Guidance Systems Via CADET," Analytical Sciences Corp., Rept. TR-385-2, May 31, 1975.

[5]Bryson, A.E. and Ho, Y.C., *Applied Optimal Control*, Blaisdell Publishing Co., Waltham, Mass., 1969.

[6]Phaneuf, R.J., "Approximate Nonlinear Estimation," Ph.D. Thesis, Massachusetts Insitute of Technology, Cambridge, Mass., May 1968.

[7]Hedrick, K.S., "The Use of Statistical Describing Functions with Linear-Quadratic-Gaussian Controller Design," *Proceedings of the 1976 Joint Automatic Control Converence*, Purdue Univ., 1976.

[8]Gelb, A. and Vander Velde, W.E., *Multiple Input Describing Functions and Nonlinear System Design*, McGraw-Hill, New York, 1963.